Miniaturized Dual-Band Bandstop Filter Using Multilayered E-Shape Microstrip Structure

Dr. Raaed T. Hammed
Department of Electrical Engineering, University of Technology, Baghdad, Iraq
Email: 30209@uotechnology.edu.iq

Received on:23/2/2016 & Accepted on:22/6/2016

ABSTRACT
This paper presents a new design technique to realize a miniaturized dual-band rejection filter based on the E-shape microstrip structure for multifunctional wireless communication systems. The filter is designed on a double layer substrate to achieve compact size. On the bottom layer, two E-shape microstrip structures are realized and coupled through a space gap, g_c, to perform the specified dual-bandstop response. The filtering response of the two bandstops is improved using a top layer substrate employing a main line stub. The main line is a half wavelength hairpin resonator. These two filter circuits are capacitivley coupled using overlapping microstrip lines. To demonstrate the proposed design technique, a multi-band bandstop filter is developed with rejection frequencies of 2.4 and 5.3 GHz Wireless local Area Network (WLAN). The filter is designed and simulated using the momentum simulator of the *Advanced Design System* (ADS) software package. The resulting filter has two second-order bandstops with four transmission poles and provides two band rejections of 25 dB and 35 dB at 2.4 GHz and 5.3 GHz respectively. The filter circuit size is very small, being of the order of about 26 mm^2 excluding the feeding ports.
Keywords: E-shape microstrip structure, dual-bandstop filter, double layer substrate, multi-band rejection filter, miniaturized filters.

INTRODUCTION
Dual-band bandstop filters are highly demanded and extremely desired in many wireless communication system applications. They are used to reject the concurrent unwanted signals at two separate frequencies. Such filters are required to meet some stringent specifications including compactness, good band rejection characteristic, high selectivity, and wideband passband performance. Considering some or all of these requirements, researchers have proposed and developed many dual-band bandstop filters using different methodologies and structures. However, miniaturized dual-band bandstop filters with excellent performance characteristics have always been a challenging task.

The dual-bandstop filters can be realized using a two-step frequency-variable transformation to the low-pass filter prototype [1]. By coupling bent short-circuited stub resonators to the main line, a multi-bandstop filter for UWB application is proposed [2]. Also, two coupled stepped impedance resonators (SIRs) are used to produce a compact dual bandstop filter [3]. Using two pairs of open stub resonators, a high selectivity dual bandstop filter with four transmission poles is achieved [4]. However, the resulted filter has a band rejection of 12 dB and poor upper pass band performance. Moreover, a wideband dual-bandstop filter using coupled and combined three-line microstrip structures is designed [5]. This filter has good rejection performance but the lower and upper pass band performance is very poor. Recently, a high rejection dual-bandstop filter based on open-circuited stub-loaded resonators is realized in [6]. Unfortunately, the filter requires a large circuit size of about 336 mm^2. Multi-mode resonators are highly popular for dual-bandstop filter design [7]. In this technique, the authors used an open and short

https://doi.org/10.30684/etj.34.11A.15
2412-0758/University of Technology-Iraq, Baghdad, Iraq

circuited stub loaded-resonator to realize a high selectivity dual-band bandstop response. Because of its characteristic of disturbing the shield current distribution in the ground plane, the defected ground structures (DGS) are widely used to design dual-bandstop filters [8-10]. These filters are small in size but the structures are somewhat complex. In order to reduce the number of couplings between the transmission line and resonators, a method to obtain and adjust two bandstops for a tuneable bandstop filter using multilayer technology is proposed [11].
In this work, a new technique is proposed to develop a miniaturized dual-band bandstop filter using the E-shape microstrip structure. The new technique employs two-layer substrate, where on the bottom layer the desired bandstops are developed using two coupled E-shape microstrip structures and on the top layer a circuit for filtering response enhancement is etched. The technique is demonstrated through the design process of a dual-band bandstop filter having center frequencies of 2.4/5.3 GHz. The response of the filter shows good performance with a very small circuit area of less than 26 mm^2.

E-Shape Microstrip Structure Analysis

The schematic diagram of the conductor pattern of the planar E-shape microstrip structure is shown in Fig. 1 (a). The structure is patterned on a grounded dielectric substrate. The structure is composed of two quarter-wave open-circuited stubs at a hairpin resonant frequency loaded by a middle stub. The stub is short-circuited at its end to the ground through a VIA hole. In the layout presented in Fig. 1 (a), the structure may be characterized by (Z_1, w_1, and $(\ell_1 + w) =$ $/4)$ for the quarter-wave open-circuited stubs and (Z_2, w_2, and ℓ_2) for the middle stub. The theoretical analysis and equivalent circuit, Fig. 1 (b), of the E- shape structure developed in [12] reveals that this structure can be assumed as two coupled resonators. The middle stub adjusts the coupling between the two resonators.

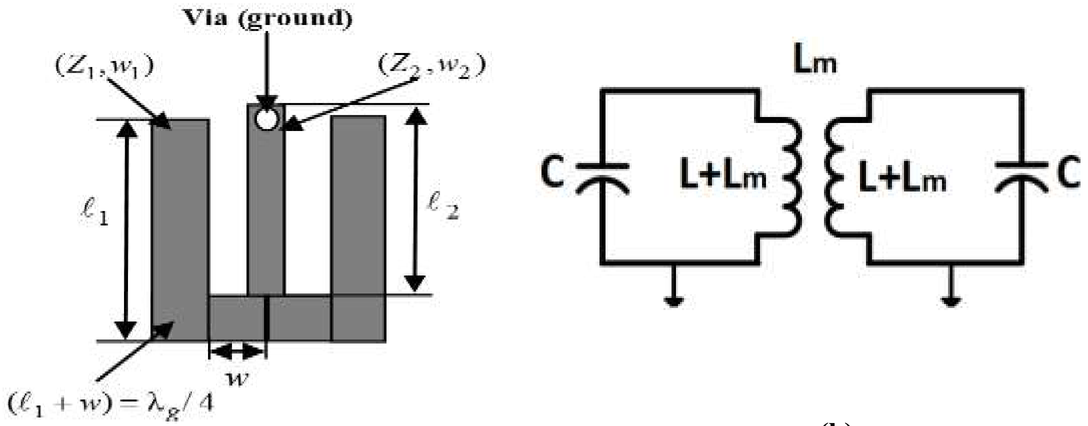

(a)

(b)

Figure(1). (a) Conductor pattern on dielectric substrate, and (b) equivalent circuit for the E-shape microstrip structure with grounded middle stub.

As shown in [12], the values of elements and C in the equivalent circuit of Fig. 1. (b) are given by the low frequency approximation (i.e: $\ell_2$and $(\ell \quad w)$ at sufficiently low frequencies). Hence, the element values are given by [13]:

$$\ell/V \qquad \ldots (1)$$

$$\ell/(Z \quad) \qquad \ldots (2)$$

where V_P, Z_o, and ℓ represent the wave velocity, characteristic impedance, and physical length of the transmission line involved in the structure respectively. The value of L in the equivalent circuit is obtained using the value of C in Eq. (2) and the resonant frequency of the hairpin resonator set by length $2(\ell_1 + w) = \lambda_g/2$. This frequency is the main resonant frequency of the E-shape microstrip structure.

Considering the equivalent circuit, Fig. 1 (b), the resonant frequency of one of the resonators (in isolation) is:

$$f_0 = \frac{1}{2\pi\sqrt{(L_m + L)C}} \qquad \ldots(3)$$

and the coupling frequencies of the two coupled resonators are:

$$f_1 = \frac{1}{2\pi\sqrt{(L_m + L + L_m)C}} = \frac{1}{2\pi\sqrt{(2L_m + L)C}} \qquad \ldots(4)$$

$$f_2 = \frac{1}{2\pi\sqrt{(L_m + L - L_m)C}} = \frac{1}{2\pi\sqrt{LC}} \qquad \ldots(5)$$

In this design, the E-shape microstrip structure is realized with two resonant frequencies, f_1=2.4 GHz and f_2=5.3 GHz. Following the above information, the E-shape microstrip structure has physical dimensions of mm, $\ell_2 = 4.3\ mm$, $w_1 = 0.45\ mm$, mm, and when the substrate of the E-shape microstrip structure has and mm. Next, the E-shape microstrip structure and its equivalent circuit are simulated using the momentum simulator of ADS [14], and their responses are plotted in Fig. 2. This figure illustrates the imaginary part of the input impedance (Z_{in}) for the E-shape microstrip structure and its equivalent circuit with respect to frequency. It is clear that the E-shape microstrip structure response has two resonant frequencies at f_1=2.4 GHz and f_2=5.3 GHz which almost agrees with its equivalent circuit behavior.

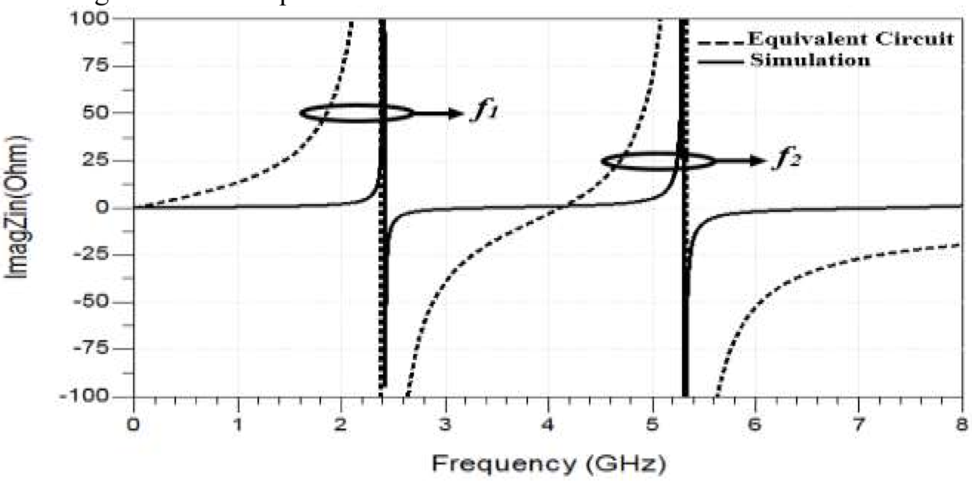

Figure(2). Impedance Response of the E-shape Microstrip Structure and its Equivalent Circuit of Fig. 1,where *C*=1.47 pF, *L*=0.61 nH, and L_m=1.23 nH.

In principle, the mutual coupling between the two resonators leads to the two coupling frequencies Eq. (4) and Eq. (5) from which the coupling coefficient (k) between the resonators can be calculated from [15]:

$$k = \frac{f_2^2 - f_1^2}{f_2^2 + f_1^2} \qquad \ldots(6)$$

Normally, the coupling coefficient is a function of the spacing between the resonators. For the E-shape microstrip structure presented in Fig. 1 (a), the coupling coefficient is a function of the length of the grounded middle stub, ℓ_2. Using the momentum simulator of ADS and equation (6), the coupling coefficients of the E-shape microstrip structure was extracted and plotted versus the coupling length (ℓ_2) with a fixed hairpin resonance frequency f_2 as shown in Fig. 3. The structure is implemented on a grounded substrate (RT Duriod 6010LM) with a dielectric constant of 10.2 and a thickness $h_1 = 0.254\ mm$. As Fig. 3 shows, the longer ℓ_2 the larger is the coupling coefficient (k).

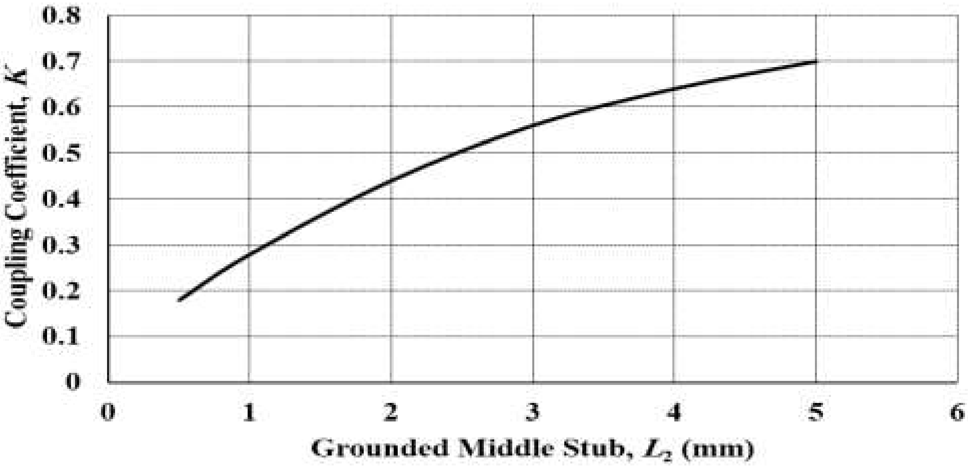

Figure(3). The Extracted Coupling Coefficient versus the Grounded Middle Stub Physical length where the hairpin resonance is fixed at $2(\ell_1 + w) = \lambda_g/2$=11.5 mm.

Dual-Band Bandstop Filter Design

To realize a dual-band bandstop filter using the E-shape microstrip structure, one can start with specifying the coupling frequencies f_1 and f_2, which are effectively the center frequencies of the desired dual-band rejection filter. In this work, a dual-band bandstop filter is developed to be used in a multifunctional wireless communication system having center frequencies of 2.4 and 5.3 GHz.

The conductor layout of the proposed filter and its equivalent circuit is shown in Fig. 4. This filter is developed on a double layer substrate. As shown in Figure 4 (a), the bottom layer employs two identical E-shape microstrip structures coupled through a space gap g_c to specify the two band rejections of the proposed filter. In the equivalent circuit, Fig. 4 (c), the space gap g_c is defined as a J-inverter with coupling capacitor C_c. On the second layer substrate shown in Fig. 4 (a), the conductor pattern of the main line signal is designed using a half wavelength hairpin resonator. These two filter circuits are capacitivley coupled using overlapping microstrip lines. The strength of the coupling coefficient between the broadside coupled lines can be controlled and adjusted through the thickness of the second dielectric layer h_2 shown in Fig. 4 (b). These capacitive couplings operate as two J-inverters (two external coupling capacitors C_e) as depicted in Fig. 4 (c), and thereby transforming the two coupled parallel resonant circuits of the E-shaped microstrip structures to two coupled series resonant circuits between the input/output and the ground, causing dual band rejection filter response.

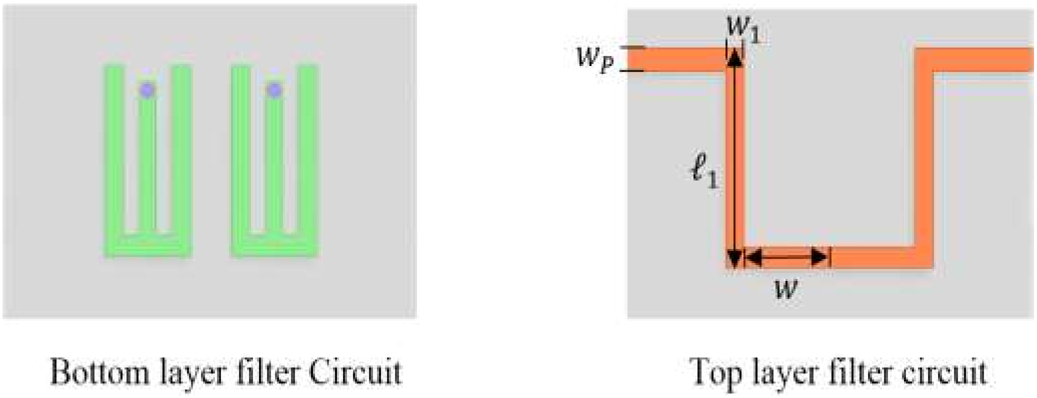

(a)

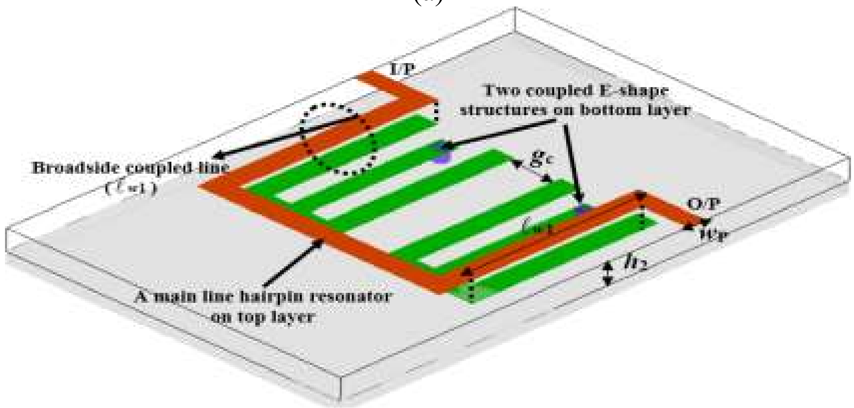

(b)

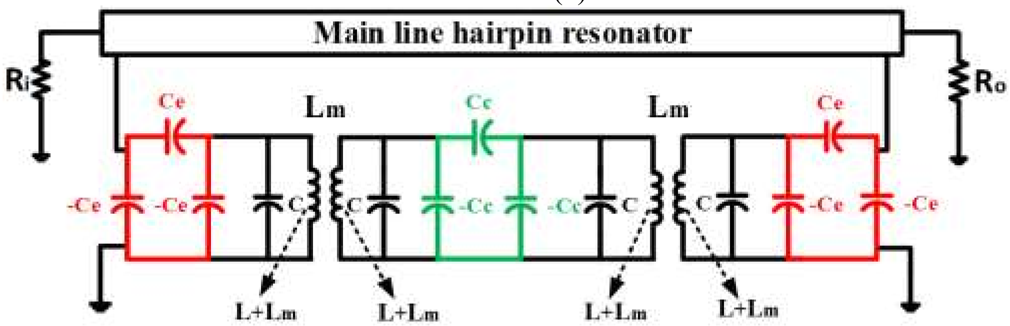

(c)

Figure 4. The Proposed Dual-Band Bandstop Filter, (a) Conductor pattren on single layer substrate, (b) Conductor pattren on multilayred substrate, and (c) Equivelant Circuit.

To implement the proposed filter circuit, the E-shape microstrip structure has been used with the same physical dimensions and electrical properties calculated previously to set the desired rejection frequencies f_1=2.4 GHz and f_2=5.3 GHz. However, due to the effect of the top layer, the design in Fig. 1 (a) needs to be retuned and therefore the line lengths ℓ_1 and ℓ_2 are refined such that $\ell_1 = 4.1\,mm$ and $\ell_2 = 3.1\,mm$ to maintain the original center frequencies f_1 and f_2. The top main line hairpin resonator is designed with physical dimensions of mm, $w_1 = 0.45\,mm$, and w and is fabricated on a Rogers RT Duriod 6010LM substrate with a dielectric constant .2 and a thickness $h_2 = 0.254\,mm$. The 50 Ω input/output ports width of w are directly connected to the top far ends of the hairpin resonator. The two circuits are capacitively coupled with broadside coupled lines having length of $\ell_{w1} = 4.1\,mm$ as shown in Fig. 4 (a). Next, the filter response is simulated and improved through the two important coupling degrees of space gap g_c and thickness h_2

using the momentum simulator of ADS. Fig. 5 illustrates the filter responses versus fixed g_c and variable h_2. From this sketch, we can see that the closer h_2 leads to stronger external coupling and thereby the filter response is enhanced. On the other hand, the filter responses are plotted against fixed h_2 and variable g_c as depicted in Fig. 6. Obviously, this figure shows that the decrease in the space gap (g_c) leads to wider band rejection at both bandstops.

However, the filter response is accomplished with two band rejections having second-order response at g_c=1 mm and h_2=0.254 mm as shown in Fig. 7. The simulated response shown in Fig. 7 (a) shows that the filter has four transmission poles leading to a high skirt selectivity with good isolation. The resulting filter exhibits an attenuation per bandwidth of 25 dB/80 MHz at 2.4 GHz and 35 dB/100 MHz at 5.3 GHz respectively. The filter has good performance at the lower, mid, and upper passbands. The filter circuit covers an area of 5.2 mm × 4.85 mm (i.e. less than 26 mm^2) excluding the feeding ports. Practically, the two circuits of the filter can be photographically etched and stacked together as one circuit. Once the prototype is ready, it can be tested and measured using a wideband universal microstrip test fixture with the aid of a vector network analyzer.

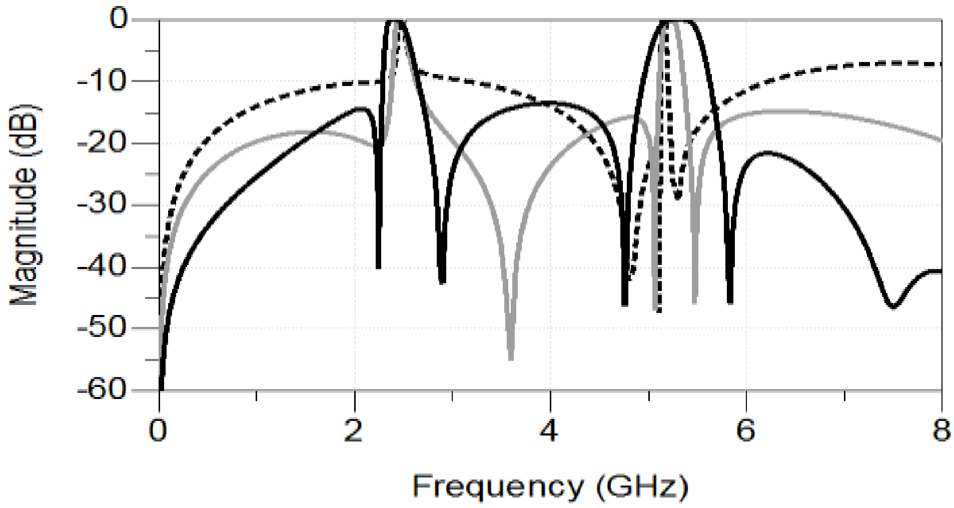

(a)

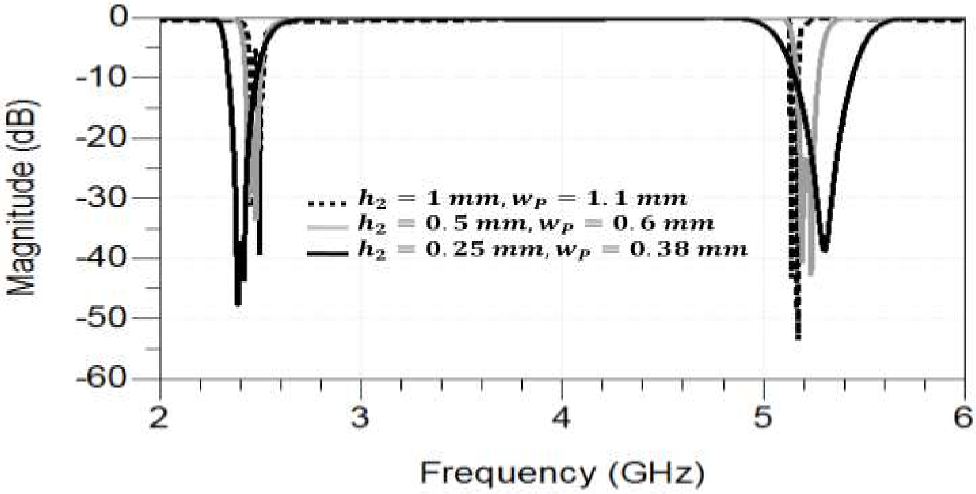

(b)

Figure (5). Simulated S-parameters of the Dual-Bandstop Filter presented in Fig. 4 with fixed $g_c = 1.5\ mm$, (a) Return Loss, and (b) Insertion Loss.

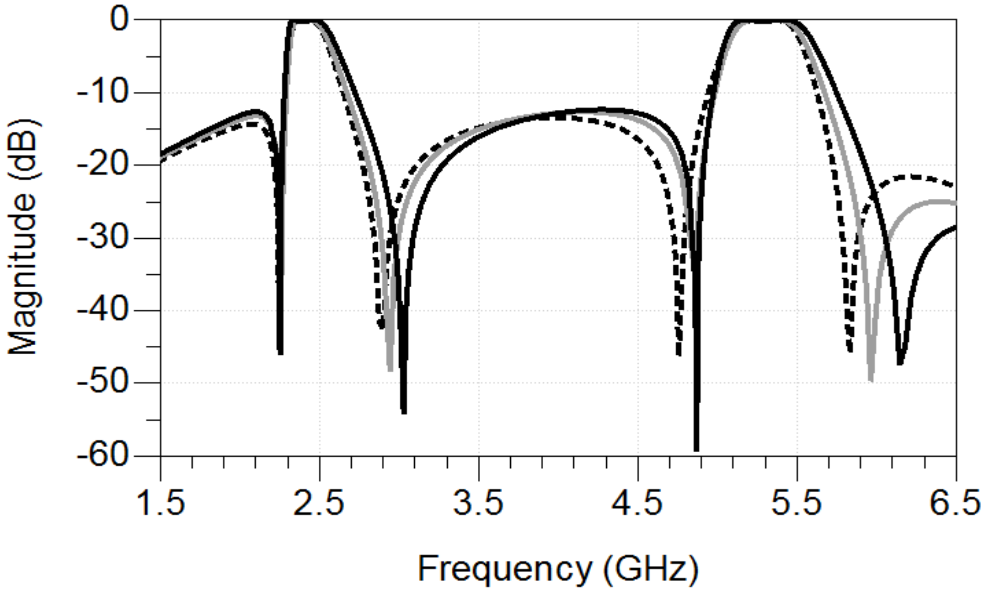

(a)

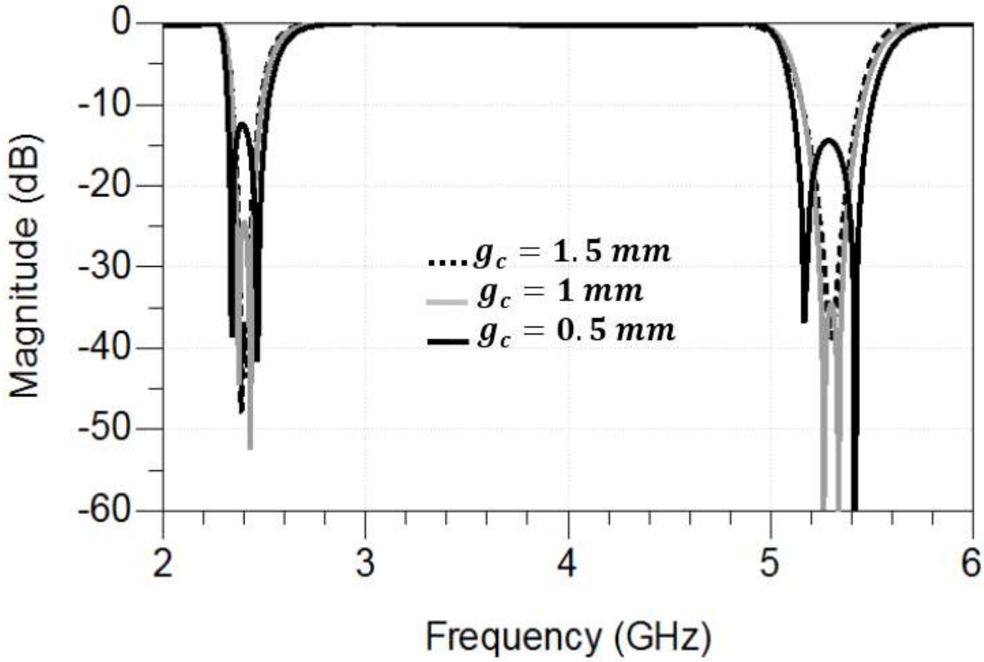

(b)

Figure(6). Simulated S-parameter of dual-bandstop filter, Fig. 4, with fixed and . (a) Return loss, and (b) Insertion loss.

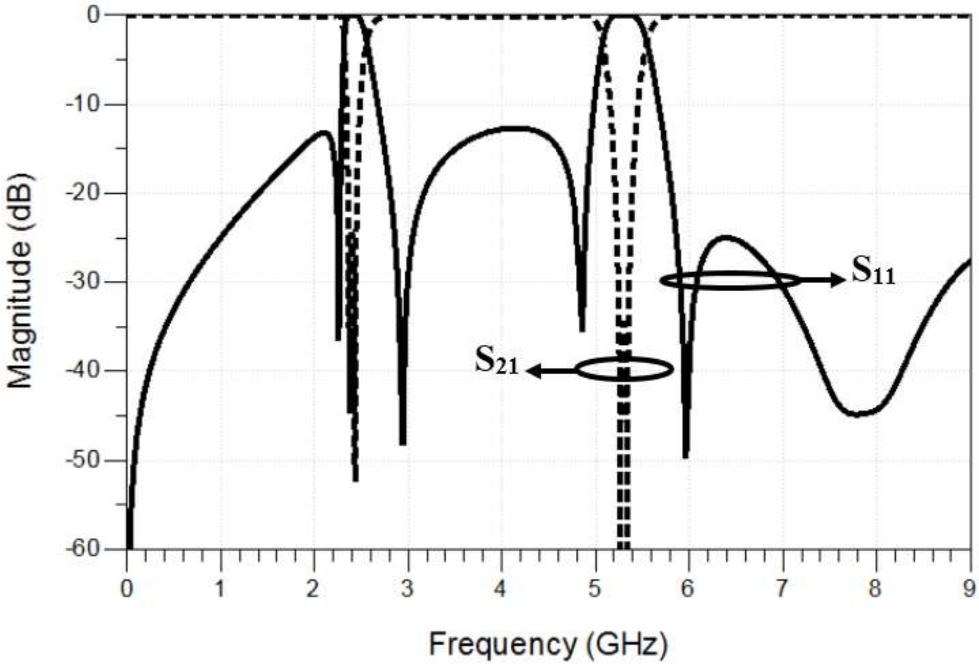

(a)

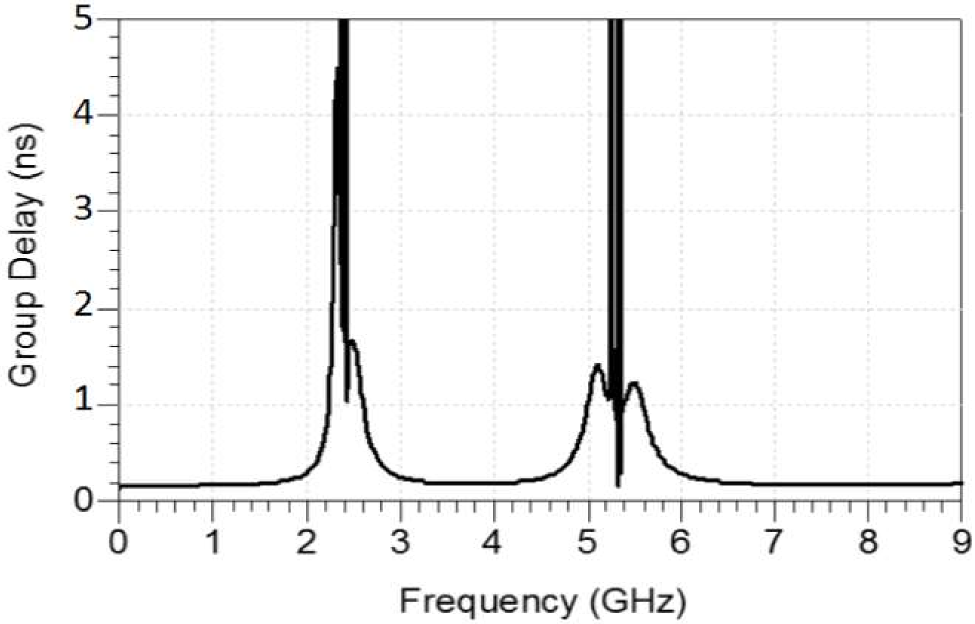

(b)

Figure(7). Simulated S-parameters of the dual-bandstop filter of Fig.4 with and *mm*. (a) Return and insertion losses, and (b) Group delay.

Table I summarizes a comparison between the proposed filter and other reported dual-band rejection filters. It is clear that the resulting filter in this work shows good performance with a very compact size.

Table (I). Performance Comparison with Different Reported Dual-Bandstop Filters

Reference	Frequency (GHz)	Attenuation Level (dB)	Passband Performance	Transmission Poles	Circuit Size (mm^2)
[4]	3.2/5.2	13/12	Good	4	900
[5]	2.1/5.3	25/20	Poor	4	252
[6]	2.4/5.2	42/44	Normal	4	336
[9]	2.71/4.97	13/18	Normal	4	36
[10]	2.4/5.8	45/45	Poor	4	150
This work	2.4/5.3	25/35	Very Good	4	26

CONCLUSION

A new design technique for developing a miniaturized dual-band bandstop filter using an E-shape microstrip structure is presented. This filter is designed based on a multilayer technology. An E-shape microstrip structure has been realized with two coupled frequencies f_1 and f_2, which are effectively the center frequencies of the desired dual-band rejection filter. Two E-shape structures have been coupled and patterned on a grounded bottom layer substrate to perform the desired passbands. The filtering response has been achieved through a second layer circuit employing a main line half wavelength hairpin resonator. The strength of the coupling coefficient between the broadside coupled lines is obtained through the thickness of the second dielectric layer (h_2). It is shown that the capacitive coupling in the layout can be considered as a J-inverter in the equivalent circuit, which transforms the E-shape microstrip structures into two series resonant circuits between the input/output and the ground and hence two bandstops are produced in the response of the filter. To demonstrate the technique and design process, a multi-band rejection filter has been developed to serve a multi-band communication system having center frequencies of 2.4/5.3 GHz. The resulting filter shows good band rejection characteristic and excellent passband performance. The filter has a very small circuit area of less than 26 mm^2 excluding the termination ports.

ACKNOWLEDGEMENT

The author would like to express his deep gratitude to Mr. Firas M. Ali for his review and useful notes concerning the manuscript of this paper.

REFERENCES

[1] H. Uchida, H. Kamino, K. Totani, N. Yoneda, M. Miyazaki, Y. Konishi, S. Makino, J. Hirokawa, and M. Ando,"Dual-band-rejection filter for distortion reduction in RF transmitters", IEEE Transaction on Microwave Theory and Techniques, vol. 52, no. 11, pp. 2550–2556, Nov. 2004.

[2] K. Rambabu, M. Chia, K. Chan, and J. Bornemann, "Design of multiple-stopband filters for interference suppression in UWB applications", IEEE Transaction on Microwave Theory and Techniques, vol. 54, no. 08, pp. 3333–3338, Aug. 2006.

[3] K. Chin, J. Yeh, and S. Chao, "Compact dual-band bandstop filters using stepped-impedance resonators," IEEE Microwave Wireless Component Letters, vol. 17, no. 12, pp. 200-202, Dec. 2007.

[4] Y. Luo and Q. Chu, "A compact high selectivity dual-band bandstop filter using bent L-resonators," Proceedings of the 43rd European Microwave Conference, Nuremberg, Germany, pp. 25-28, Oct. 2013.

[5] T. Faraji, and R. Hazeri, "Microstrip dual-band bandstop filter to supress DGS, DMB, GPS, UTMTS, WCDMA, WIBRO, and WLAN bands," Microwave and Optical Technology Letters, vol. 54, no. 04, pp. 854-856, April 2012.

[6] F. Chen, J. Qiu, and Q. Chu "Dual-band bandstop filter using stub-loaded resonators with sharp rejection characteristic," Electronics Letters, vol. 49, no. 05, pp. 351-353, Feb. 2013.

[7] L. Gao, S. Cai, X. Zhang, and Q. Xue, "Dual-band bandstop filter using open and short stub-loaded resonators," International conference on Microwave and Millimetre Wave Technology, Shenzhen, China, pp. 1-3, May 2012.
[8] J. Wang, H. Ning, L. Mao, and M. Li, "Miniaturized dual-band bandstop filter using defected microstrip structure and defected ground structure," IEEE MTT-S International Microwave Symposium Digest, Montreal, Canada, pp. 1-3, Jun 2012.
[9] J. Xiao, and Y. Zhu, "Multi-band bandstop filter using inner T-shaped defected microstrip structure (DMS)," International Journal of Electronics and Communications, vol. 68, no. 2, pp. 90-96, Feb. 2014.
[10] I. Sassi, L. Talbi, and K. Hettak, "Compact multi-band filter based on multi-Ring complementary split ring resonators," Progress in Electromagnetics Research C, pp. 127-135, May 2015.
[11] K. Lee, T. Lee, C. Ahnand, Y. Kim, and J. Lee, "Reconfigurable dual-stopband filters with reduced number of couplings between a transmission line and resonators," IEEE Microwave Wireless Component Letters, vol. 25, no. 02, pp. 106-108, Feb. 2015.
[12] R. Hammed and D. Mirshekar-Syahkal, "A lumped element equivalent circuit of E-shape microstrip structure for UWB filter design," Proceedings of the 41st European Microwave Conference, Manchester, UK, pp. 651-654, Oct. 2011.
[13] J. S. Hong and M. J. Lancaster, Microstrip Filters for RF/Microwave Applications, New York: Wiley, 2001.
[14] Advanced Design System (ADS) 2008A, Agilent Technologies, Palo Alto, CA, USA, 2009.
[15] J. S. Hong and M. J. Lancaster, "Couplings of microstrip square open-loop resonators for cross-coupled planar microwave filters," IEEE Transactions on Microwave Theory and Techniques, vol. 44, no. 12, pp. 2099-2109, Dec. 1996.